doi:10.1093/brain/awaa188 BRAIN 2020: Page 1 of 17 | 1

BRAIN
A JOURNAL OF NEUROLOGY

Structural connectivity predicts clinical outcomes of deep brain stimulation for Tourette syndrome

Kara A. Johnson,[1,2] Gordon Duffley,[1,2] Daria Nesterovich Anderson,[1,2,3] Jill L. Ostrem,[4] Marie-Laure Welter,[5] Juan Carlos Baldermann,[6,7] Jens Kuhn,[6,8] Daniel Huys,[6] Veerle Visser-Vandewalle,[9] Thomas Foltynie,[10] Ludvic Zrinzo,[10] Marwan Hariz,[10,11] Albert F.G. Leentjens,[12] Alon Y. Mogilner,[13] Michael H. Pourfar,[13] Leonardo Almeida,[14] Aysegul Gunduz,[14,15] Kelly D. Foote,[14] Michael S. Okun[14] and Christopher R. Butson[1,2,3,16]

Deep brain stimulation may be an effective therapy for select cases of severe, treatment-refractory Tourette syndrome; however, patient responses are variable, and there are no reliable methods to predict clinical outcomes. The objectives of this retrospective study were to identify the stimulation-dependent structural networks associated with improvements in tics and comorbid obsessive-compulsive behaviour, compare the networks across surgical targets, and determine if connectivity could be used to predict clinical outcomes. Volumes of tissue activated for a large multisite cohort of patients ($n = 66$) implanted bilaterally in globus pallidus internus ($n = 34$) or centromedial thalamus ($n = 32$) were used to generate probabilistic tractography to form a normative structural connectome. The tractography maps were used to identify networks that were correlated with improvement in tics or comorbid obsessive-compulsive behaviour and to predict clinical outcomes across the cohort. The correlated networks were then used to generate 'reverse' tractography to parcellate the total volume of stimulation across all patients to identify local regions to target or avoid. The results showed that for globus pallidus internus, connectivity to limbic networks, associative networks, caudate, thalamus, and cerebellum was positively correlated with improvement in tics; the model predicted clinical improvement scores ($P = 0.003$) and was robust to cross-validation. Regions near the anteromedial pallidum exhibited higher connectivity to the positively correlated networks than posteroventral pallidum, and volume of tissue activated overlap with this map was significantly correlated with tic improvement ($P < 0.017$). For centromedial thalamus, connectivity to sensorimotor networks, parietal-temporal-occipital networks, putamen, and cerebellum was positively correlated with tic improvement; the model predicted clinical improvement scores ($P = 0.012$) and was robust to cross-validation. Regions in the anterior/lateral centromedial thalamus exhibited higher connectivity to the positively correlated networks, but volume of tissue activated overlap with this map did not predict improvement ($P > 0.23$). For obsessive-compulsive behaviour, both targets showed that connectivity to the prefrontal cortex, orbitofrontal cortex, and cingulate cortex was positively correlated with improvement; however, only the centromedial thalamus maps predicted clinical outcomes across the cohort ($P = 0.034$), but the model was not robust to cross-validation. Collectively, the results demonstrate that the structural connectivity of the site of stimulation are likely important for mediating symptom improvement, and the networks involved in tic improvement may differ across surgical targets. These networks provide important insight on potential mechanisms and could be used to guide lead placement and stimulation parameter selection, as well as refine targets for neuromodulation therapies for Tourette syndrome.

1 Scientific Computing and Imaging Institute, University of Utah, Salt Lake City, Utah, USA
2 Department of Biomedical Engineering, University of Utah, Salt Lake City, Utah, USA
3 Department of Neurosurgery, University of Utah, Salt Lake City, Utah, USA
4 Department of Neurology, University of California San Francisco, San Francisco, California, USA

Received October 25, 2019. Revised March 12, 2020. Accepted April 20, 2020

5 Institut du Cerveau et de la Moelle Epiniere, Sorbonne Universités, University of Pierre and Marie Curie University of Paris, the French National Institute of Health and Medical Research U 1127, the National Center for Scientific Research 7225, Paris, France
6 Department of Psychiatry and Psychotherapy, University of Cologne, Cologne, Germany
7 Department of Neurology, University of Cologne, Cologne, Germany
8 Department of Psychiatry, Psychotherapy, and Psychosomatic Medicine, Johanniter Hospital Oberhausen, EVKLN, Oberhausen, Germany
9 Department of Stereotaxy and Functional Neurosurgery, University Hospital Cologne, Cologne, Germany
10 Functional Neurosurgery Unit, Department of Clinical and Movement Neurosciences, University College London, Queen Square Institute of Neurology, London, UK
11 Department of Clinical Neuroscience, Umea University, Umea, Sweden
12 Department of Psychiatry and Neuropsychology, Maastricht University Medical Center, Maastricht, The Netherlands
13 Center for Neuromodulation, New York University Langone Medical Center, New York, New York, USA
14 Norman Fixel Institute for Neurological Diseases, Program for Movement Disorders and Neurorestoration, Departments of Neurology and Neurosurgery, University of Florida, Gainesville, Florida, USA
15 J Crayton Pruitt Family Department of Biomedical Engineering, University of Florida, Gainesville, Florida, USA
16 Departments of Neurology and Psychiatry, University of Utah, Salt Lake City, Utah, USA

Correspondence to: Christopher R. Butson
Scientific Computing and Imaging Institute, 72 S Central Campus Drive, Room 3686
Salt Lake City, UT 84112, USA
E-mail: butson@sci.utah.edu

Keywords: neuromodulation; tics; obsessive-compulsive behaviour; cortico-striato-thalamo-cortical networks; tractography

Abbreviations: CMn = centromedian nucleus; DBS = deep brain stimulation; GPi = globus pallidus internus; HCP = Human Connectome Project; OCB = obsessive-compulsive behaviour; RCT = randomized controlled trial; VTA = volume of tissue activated; Y-BOCS = Yale-Brown Obsessive-Compulsive Scale; YGTSS = Yale Global Tic Severity Scale

Introduction

Tourette syndrome is a neurodevelopmental disorder characterized by motor and vocal tics (Leckman, 2002). Tourette syndrome is often associated with comorbid behavioural and psychiatric disorders, including attention-deficit disorders and obsessive-compulsive behaviour (OCB) (Hirschtritt *et al.*, 2015). The underlying pathophysiology of Tourette syndrome is generally thought to involve dysfunction within cortico-striato-thalamo-cortical (CSTC) networks (Leckman *et al.*, 1997; Mink, 2001). The complex interaction of motor and psychiatric symptoms and evidence from neuroimaging studies indicate that Tourette syndrome pathophysiology involves CSTC networks that span many different functions, including sensorimotor networks (primary motor cortex, primary sensory cortex, premotor regions, and supplementary motor area), limbic networks (cingulate cortex and orbitofrontal cortex), associative networks (prefrontal cortex), parietal-temporal-occipital networks, as well as the basal ganglia, thalamus, and cerebellum (Thomalla *et al.*, 2009; Draganski *et al.*, 2010; Tobe *et al.*, 2010; Worbe *et al.*, 2010, 2015; Müller-Vahl *et al.*, 2014; Neuner *et al.*, 2014). Despite increasing knowledge about network impairments associated with Tourette syndrome, it remains unknown which specific networks should be modulated in order to improve Tourette syndrome and its comorbidities.

Deep brain stimulation (DBS) has been shown to alleviate symptoms in select patients with treatment-refractory Tourette syndrome. Since the first case report in 1999 (Vandewalle *et al.*, 1999), over 270 patients with Tourette syndrome have been implanted with DBS with an average of 40% improvement in tics, as well as overall improvements in quality of life (Huys *et al.*, 2016; Martinez-Ramirez *et al.*, 2018). Based on the model of CSTC dysfunction, the most common target regions for Tourette syndrome DBS are regions within the centromedial thalamus and the globus pallidus internus (GPi). The majority of studies have been open-label trials, but some randomized controlled trials (RCTs) of small cohorts have reported significant tic reduction during active DBS compared to sham, indicating that DBS may be a viable therapy for select patients with Tourette syndrome with positive long-term outcomes (Ackermans *et al.*, 2011; Kefalopoulou *et al.*, 2015; Welter *et al.*, 2019). Other RCTs have reported no significant decrease in tics, possibly due to insufficient follow-up time (Welter *et al.*, 2017). Although DBS shows promise as a therapy for Tourette syndrome, outcomes vary substantially across patients, and reliable predictors of therapeutic response have not been identified. Recently, our multisite study of a large cohort of patients found that the location of stimulation relative to structural neuroanatomy did not fully explain the variability in outcomes of DBS for Tourette syndrome (Johnson *et al.*, 2019). Therefore, there remains a critical need for a reliable predictor of clinical outcomes to improve understanding of how the therapeutic response to DBS is mediated.

The therapeutic effects of DBS for Tourette syndrome are likely derived from a complex combination of how stimulation modulates both local brain regions and distributed networks that are connected to the site of stimulation. However, the few studies investigating network-level effects have been limited to small cohorts. A recent study of five subjects reported that structural connectivity of the site of stimulation in the centromedial thalamus to the right middle frontal gyrus, the left frontal superior sulci region, and the left cingulate sulci region was correlated with tic improvement (Brito *et al.*, 2019). Additionally, stimulation of the centromedial thalamus or posteroventral GPi seems to affect distributed cortical and subcortical regions (Haense *et al.*, 2016), and specific components of frontostriatal, limbic, and motor networks were correlated with tic improvements (Jo *et al.*, 2018). The preliminary evidence from these studies suggests that the connectivity profile of the stimulation site may be related to clinical outcomes of DBS for Tourette syndrome; however, it has yet to be determined whether connectivity to these networks is predictive of outcomes in a large cohort of patients. Additionally, it is unknown whether there are common therapeutic networks that mediate the improvement in tics or comorbidities across surgical targets. As a result, it remains unclear which networks are reliably associated with clinical improvement or how future studies could leverage these networks to target more effectively. It is imperative to identify the networks that mediate the therapeutic effects, as they could guide the development of new brain targets or refinement of established targets in order to improve invasive and non-invasive neuromodulation therapies for Tourette syndrome.

The present study expands on previous research from the International Tourette Syndrome DBS Registry and Database by incorporating normative connectome data to generate predictive models based on the structural connectivity of the site of stimulation (Horn *et al.*, 2017). The objectives were to identify the structural networks that were correlated with improvements in tics and OCB following DBS of the centromedial thalamus or GPi, compare these networks across the two targets, and determine if connectivity could be used to predict clinical outcomes. Further, we aimed to use these structural networks to parcellate the total volume of stimulation across all patients into regions connected to positively correlated networks versus negatively correlated networks in order to adapt the distributed connectivity maps into local maps that could be used to guide the therapy. We hypothesized that beneficial effects of DBS would be associated with connectivity to specific regions involved in CSTC networks, and that connectivity profiles of patient-specific sites of stimulation could be used to predict outcomes. We further hypothesized that the DBS target regions could be parcellated into target and avoidance regions based on connectivity of the networks associated with improvements in tics and OCB. The findings of this study could be used to guide targeting and stimulation programming to better improve tics and comorbidities in patients undergoing DBS therapy for Tourette syndrome.

Materials and methods

Patient data

Retrospective data were collected from patients implanted in bilateral centromedial thalamus or GPi who were included in the International Tourette Syndrome DBS Database and Registry (https://tourettedeepbrainstimulationregistry.ese.ufhealth.org/) in collaboration with the International Neuromodulation Registry (https://neuromodulationregistry.org/). The cohort is a subset of the patients included in our previously published analysis (Johnson *et al.*, 2019). We note that the GPi cohort was not subdivided by the intended target subregion (anteromedial versus posteroventral) because our previous study showed that many stimulation volumes spanned multiple subregions of GPi. The dataset included pre- and postoperative imaging (MRI, CT), baseline clinical rating scale scores, clinical rating scale scores at latest follow-up, and stimulation settings at latest follow-up. The clinical rating scales included the Yale Global Tic Severity Scale (YGTSS) (Leckman *et al.*, 1989) and the Yale-Brown Obsessive-Compulsive Scale (Y-BOCS) (Goodman *et al.*, 1989). The baseline and follow-up scores were used to calculate the per cent improvement in symptoms compared to baseline before DBS surgery.

Preprocessing of patient imaging

The details of image preprocessing for each patient were previously described in detail (Johnson *et al.*, 2019). In brief, the bilateral DBS leads were localized in the postoperative MRI or CT for each patient manually using SCIRun software [v4.7, Scientific Computing and Imaging (SCI) Institute, University of Utah, Salt Lake City, UT, http://sci.utah.edu/software/scirun.html]. The postoperative MRI or CT was aligned to the preoperative MRI for each patient using automated rigid registration in 3D Slicer software (Fedorov *et al.*, 2012) (http://www.slicer.org). The skull-stripped preoperative MRI for each patient was aligned to the Montreal Neurological Institute (MNI) 2009*b* Nonlinear Asymmetric Atlas using non-linear registration implemented in ANTs software (Avants *et al.*, 2008). As a result, we obtained transformations for each patient's lead locations into the MNI atlas space to facilitate comparisons across patients.

Estimation of the volume of tissue activated

The volume of tissue activated (VTA) is an estimation of the effects of DBS on the tissue surrounding the electrode (Butson *et al.*, 2007, 2011). Bilateral VTAs were estimated for each patient using the stimulation parameters from the latest follow-up time point. First, a finite element mesh and bioelectric field solutions were calculated for the Medtronic 3387, Medtronic 3389, and NeuroPace DL-330-3.5 electrodes using SCIRun v4.7. A geometric model of each electrode was placed in a $100 \times 100 \times 100$ mm volume, and a subgrid of $20 \times 20 \times 20$ mm at 0.1 mm resolution was centrally placed around the stimulation contacts for each lead. A tetrahedral mesh was created using the TetGen module in SCIRun; finite element meshes comprised approximately 50–60 million elements. Contacts were modelled as ideal conductors, and electrode shafts were

modelled as ideal insulators (Vorwerk *et al.*, 2019). Unit bioelectric field solutions were solved at –1 V for each lead contact with Dirichlet boundary conditions of 0 V set on the volume boundary to simulate a distant return electrode. Tissue conductivity was set to 0.2 S/m, and a 0.5-mm encapsulation layer was included with its conductivity set to 0.1 S/m, corresponding to a medium impedance state (Butson *et al.*, 2006).

As previously described (Anderson *et al.*, 2018), the Hessian matrix of second derivatives can be used to approximate neural activation based on thresholds of the second derivative established from computational axon models (Rattay, 1986, 1999). The advantage of using the Hessian matrix to estimate the effects of stimulation is that it accounts for all possible fibre orientations, which was appropriate for this analysis since we were mapping connectivity based on fibre pathways. The Hessian matrix was calculated at each point on the subgrid, and the primary eigenvector, which represents the most excitable orientation of axon activation, was calculated through eigenvalue decomposition of the Hessian matrix (Anderson *et al.*, 2019). Because of the principle of linearity, unit bioelectric solutions were scaled based on voltage parameters of individual patient DBS settings or summed if multiple contacts were used, such as in bipolar configurations. Second derivative firing thresholds of axons have been previously identified, and threshold values were chosen based on patient-specific stimulation parameters (Duffley *et al.*, 2019). The VTAs were generated by thresholding the maximum eigenvalue, warped using each patient's set of transformations from their lead locations in native imaging space to MNI atlas space, and used as seed regions for tractography.

Normative structural connectome

Diffusion-weighted imaging

A normative tract probability map was created for each VTA using diffusion-weighted imaging (DWI) acquired in 40 healthy, unrelated subjects in the Human Connectome Project (HCP) Young Adult dataset (Van Essen *et al.*, 2008). The healthy subjects cohort was selected randomly and included 22 female/18 male subjects belonging to a distribution of age groups (22–25 years: $n = 4$; 26–30 years: $n = 18$; 31–35 years: $n = 18$). The imaging was preprocessed using the HCP minimal preprocessing pipeline, which includes registration to the MNI atlas and DWI distortion correction methods (Glasser *et al.*, 2013). Also as part of the HCP preprocessing pipeline, the FMRIB Diffusion Toolbox's BEDPOSTX algorithm in FSL was used to estimate probability distributions for multiple fibre orientations at each voxel using a three-fibre model (Behrens *et al.*, 2007).

'Forward' probabilistic tractography of the volume of tissue activated

An overview of our methodological approach for generating the predictive models is shown in Fig. 1. Each VTA was used as a seed to generate probabilistic tractography in each of the HCP subjects' imaging using the probtrackx2 algorithm in FSL (Behrens *et al.*, 2007). A binary volume with 1 mm^3 voxels in MNI space was created for each VTA to be used for seeding. Overall, we generated 40 tract probability maps per VTA (one map per HCP subject), which were averaged across HCP subjects to create one average tract probability map per VTA. To generate the tract probability maps, the following default parameters were used: 5000 samples per voxel, a step length of 0.5 mm, a maximum of 2000 steps, a curvature threshold of 0.2, a subsidiary fibre volume threshold of 0.01, and pathways that looped back on themselves were discarded. The cortical grey matter ribbon segmented from each subject's structural MRI using FreeSurfer software (Fischl, 2012) was used as the 'waypoint' mask. The tract probability maps were normalized by the total number of generated fibres that met the inclusion criteria in order to account for differences in VTA volumes. To create a combined bilateral tract probability map for each patient, the left and right average tract probability maps were summed (Fig. 1A).

Statistical analysis and predictive models

Statistical analysis of clinical outcomes

A detailed statistical analysis of the long-term clinical outcomes of this cohort has been reported in our previous analysis, including analyses across targets and clinical covariates (Johnson *et al.*, 2019). In the present study, cohort characteristics were summarized using descriptive statistics, including age at surgery, sex, baseline and follow-up clinical rating scale scores, per cent improvement scores, and mean time since surgery at the final follow-up time point.

Voxelwise regression and cross-validation

To identify the networks that were correlated with clinical improvement, we performed a voxelwise linear regression of the tract probability maps across patients and their associated per cent improvement scores (Fig. 1B). Using the voxelwise linear regression map, a per cent improvement score for each patient was predicted by performing a correlation of the patient's tract probability map and the 'ideal' connectivity map (Horn *et al.*, 2017). The 'ideal' connectivity map was created by assigning each positively correlated voxel ($R > 0$) with the maximum connectivity value and each negatively correlated voxel ($R < 0$) with the minimum connectivity value across the cohort. The predicted correlation coefficients were then mapped to the range of clinical per cent improvement scores to obtain a predicted improvement score. Leave-one-out cross-validation was used to minimize overfitting of the voxelwise linear regression model and verify that the model could significantly predict outcomes for out-of-sample data. In the leave-one-out cross-validation, n voxelwise linear regression iterations were performed, where n is the number of patients in the cohort ($n = 34$ patients implanted in GPi; $n = 32$ patients implanted in centromedial thalamus). The predicted improvement score for the left-out patient was based on the 'ideal' connectivity map generated without the left-out patient. To determine if the model was predictive, a correlation of the predicted per cent improvement scores and the clinical per cent improvement scores was performed. For all statistical analyses, $P < 0.05$ was used as the threshold for statistical significance.

'Reverse' probabilistic tractography to parcellate the stimulated regions

The voxelwise regression analysis was designed to identify which networks connected to the VTA were correlated with symptom improvement. However, this map of distributed networks did not provide information about which local regions

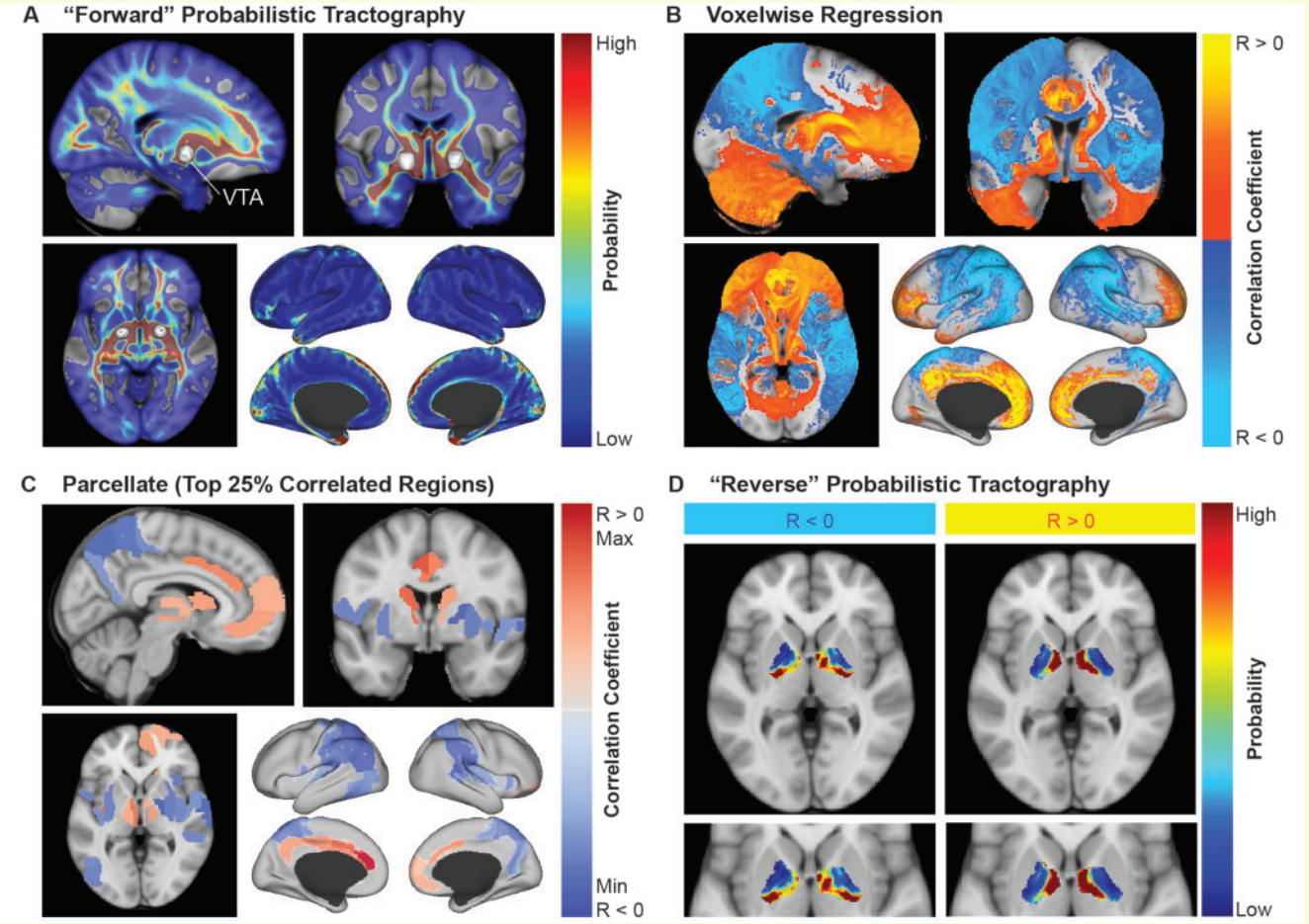

Figure 1 Overview of the methodological approach. (**A**) The bilateral VTAs for each patient (n = 66) were used to generate probabilistic tractography maps averaged over 40 HCP subjects. (**B**) Voxelwise regression was performed to identify voxels that were positively correlated ($R > 0$) or negatively correlated ($R < 0$) with outcome scores. These correlation maps were used to predict clinical outcome scores. (**C**) The maps from **B** were parcellated into the top 25% correlated regions. (**D**) The positively correlated regions and negatively correlated regions from **C** were used to generate 'reverse' probabilistic tractography to parcellate the total volume of stimulation across all patients into areas connected to positively correlated networks and areas connected to negatively correlated networks.

exhibit particular connectivity profiles. We performed an analysis to characterize which regions within the total stimulation volume across patients may result in modulation of networks that were positively or negatively correlated with outcomes. First, to create seed regions for tractography, the correlation maps that predicted clinical outcomes and survived leave-one-out cross-validation were parcellated into brain regions based on the Brainnetome atlas (cortical and subcortical areas) (Fan *et al.*, 2016) and the Mindboggle atlas (cerebellum, brainstem, and basal forebrain) (Klein and Tourville, 2012) in MNI space as distributed in the open-source software Lead-DBS (Horn and Kühn, 2015). For each patient, the average connectivity within each parcellation region was computed using their stimulation-dependent connectivity map. Next, univariate linear regression feature selection implemented in scikit-learn (Pedregosa *et al.*, 2011) was used to compute the correlation between the average connectivity and per cent improvement scores for each region and select the regions with the top 25% highest F-scores (64 regions) independent of testing for statistical significance. The associated F-scores, correlation coefficients, and false discovery rate (FDR)-corrected P-values (q-values) were reported for each set of regions. These regions were visualized (Fig. 1C) and binarized into masks assigned as positively correlated or negatively correlated with improvement. The binary masks were used as seeds for probabilistic tractography in the 40 HCP subjects using the same parameters as the VTA seeding previously described; the only difference was that a mask of the total stimulation volume, or the union of the discretized VTAs, was used as the 'waypoint' in order to exclude all tracts that did not intersect with the total stimulation volume (Fig. 1D). Maps of the ratio of the average connectivity of the positively correlated regions versus the negatively correlated regions were generated to visualize the distribution of these connectivity profiles within the total stimulation volume across patients. The maps were visualized along with segmentations of nuclei of interest from the DBS Intrinsic AtLas (DISTAL) (Ewert *et al.*, 2017). The average ratio value for each patient's VTA was calculated to

determine if the overlap of the VTA with this positive-to-negative ratio map was correlated with clinical outcomes.

Data availability

The data that support the findings of this study can be made available upon reasonable request for researchers who meet the criteria for access to International Neuromodulation Registry (https://neuromodulationregistry.org).

Results

Patient cohort

The cohort included 66 patients with Tourette syndrome who were implanted with bilateral DBS in the GPi ($n = 34$ patients; 68 leads) or the centromedial thalamus ($n = 32$ patients; 64 leads). The implanted lead models included Medtronic 3387 ($n = 37$ patients), Medtronic 3389 ($n = 24$ patients), or NeuroPace DL-330-3.5 ($n = 5$ patients). The cohort characteristics and baseline and follow-up YGTSS and Y-BOCS scores at the latest time point are shown in Table 1. The mean ± standard deviation (SD) follow-up time since DBS surgery was 24.6 ± 17.0 months. Across both targets, YGTSS total scores improved by 43.6 ± 28.9%, and Y-BOCS total scores improved by 23.6 ± 52.1%. A detailed statistical analysis of long-term clinical outcomes of this cohort was reported in our previous analysis, including clinical covariates, analyses across targets, and Kaplan-Meier curves of the time required to reach clinical response criteria (Johnson *et al.*, 2019). Active contact locations and the spatial distribution of the VTAs across the cohort were also reported in the previous study.

Structural networks correlated with improvement in tics

Maps of the voxelwise regression correlation coefficients of stimulation-dependent structural connectivity correlated with per cent improvement in YGTSS total score across patients implanted in the GPi or centromedial thalamus are shown in Fig. 2. Across patients implanted in GPi ($n = 34$) (Fig. 2A), the predicted per cent improvement scores were significantly correlated with the clinical per cent improvement scores {R = 0.49 [95% confidence interval (CI): 0.19 to 0.71], $P = 0.003$}, and leave-one-out cross-validation significantly predicted clinical outcome scores for left-out patients (R = 0.37, $P = 0.032$). The maps showed that per cent improvement in tics was positively correlated with structural connectivity to regions involved in limbic and associative networks, including the cingulate cortex, anterior prefrontal cortex, dorsomedial and dorsolateral prefrontal cortex, and orbitofrontal cortex. Connectivity to the cerebellum, caudate, and regions in the thalamus was also positively correlated with tic improvement. In contrast, connectivity to sensorimotor networks was negatively correlated, such as the primary motor cortex, primary sensory cortex, supplementary motor area, parietal-temporal-occipital regions, and putamen. Example connectivity profiles for a responder and non-responder are shown in Fig. 3A and B, which demonstrate the importance of higher connectivity to regions in the prefrontal cortex and lower connectivity to sensorimotor regions. The top correlated anatomical regions are visualized in Supplementary Fig. 1A, and the associated regression statistics are summarized in Supplementary Table 1.

The correlation maps across patients implanted in the centromedial thalamus ($n = 32$) showed mainly inverted patterns compared to GPi (Fig. 2B). Connectivity to sensorimotor networks was positively correlated with improvement in tics, including the primary motor cortex, primary sensory cortex, supplementary motor area, and putamen, as well as parietal-temporal-occipital networks. Additionally, connectivity to the cerebellum was positively correlated with improvement, which was one of the few similarities observed when comparing the maps for GPi versus centromedial thalamus. The negatively correlated networks included regions involved in limbic and associative networks, such as the cingulate cortex, prefrontal cortex, and orbitofrontal cortex. The predicted per cent improvement scores for patients were significantly correlated with the clinical per cent improvement scores [R = 0.44 (95% CI: 0.11 to 0.68), $P = 0.012$]. Leave-one-out cross-validation showed that the model significantly predicted clinical outcome scores for the out-of-sample patients (R = 0.39, $P = 0.028$). Example connectivity profiles (Fig. 3C and D) demonstrate that a responder had higher connectivity to sensorimotor networks, while a non-responder showed low connectivity to sensorimotor networks and higher connectivity to prefrontal areas. Regression statistics are summarized for the top correlated anatomical regions in Supplementary Table 2, and the regions are visualized in Supplementary Fig. 1B.

Structural networks correlated with improvement in obsessive-compulsive behaviour

Maps of the voxelwise regression correlation coefficients of stimulation-dependent structural connectivity correlated with per cent improvement in Y-BOCS total score across patients implanted in the GPi ($n = 24$) or centromedial thalamus ($n = 16$) are shown in Fig. 4. The correlation maps for patients implanted in the GPi (Fig. 4A) and for patients implanted in the centromedial thalamus (Fig. 4B) showed similar trends: connectivity to regions involved in limbic and associative networks was positively correlated with OCB improvement, including the anterior prefrontal cortex, orbitofrontal cortex, dorsomedial prefrontal cortex, and dorsolateral prefrontal cortex. Negatively correlated networks included sensorimotor networks and parietal-

Table 1 Baseline cohort data and follow-up clinical outcomes

	All patients	DBS target	
		GPi	Centromedial thalamus
Patients, *n*	66	34	32
Age at surgery (years)	29.8 (9.9)	29.4 (9.7)	30.3 (10.2)
Sex, male/female	45/21	25/9	20/12
Outcome: YGTSS total score			
Number of patients with scores	66	34	32
Baseline score	75.3 (20.9)	76.9 (20.4)	73.8 (21.6)
Follow-up score	42.7 (24.7)	42.0 (22.7)	43.4 (27.1)
% Improvement	43.6 (28.9)	45.5 (26.4)	41.6 (31.6)
Outcome: Y-BOCS total score			
Number of patients with scores	40	24	16
Baseline score	21.9 (9.0)	24.6 (9.2)	17.9 (7.3)
Follow-up score	15.3 (8.2)	16.8 (7.6)	13.1 (8.8)
% Improvement	23.6 (52.1)	23.2 (57.7)	24.1 (44.1)

Values are mean (SD) unless otherwise noted.

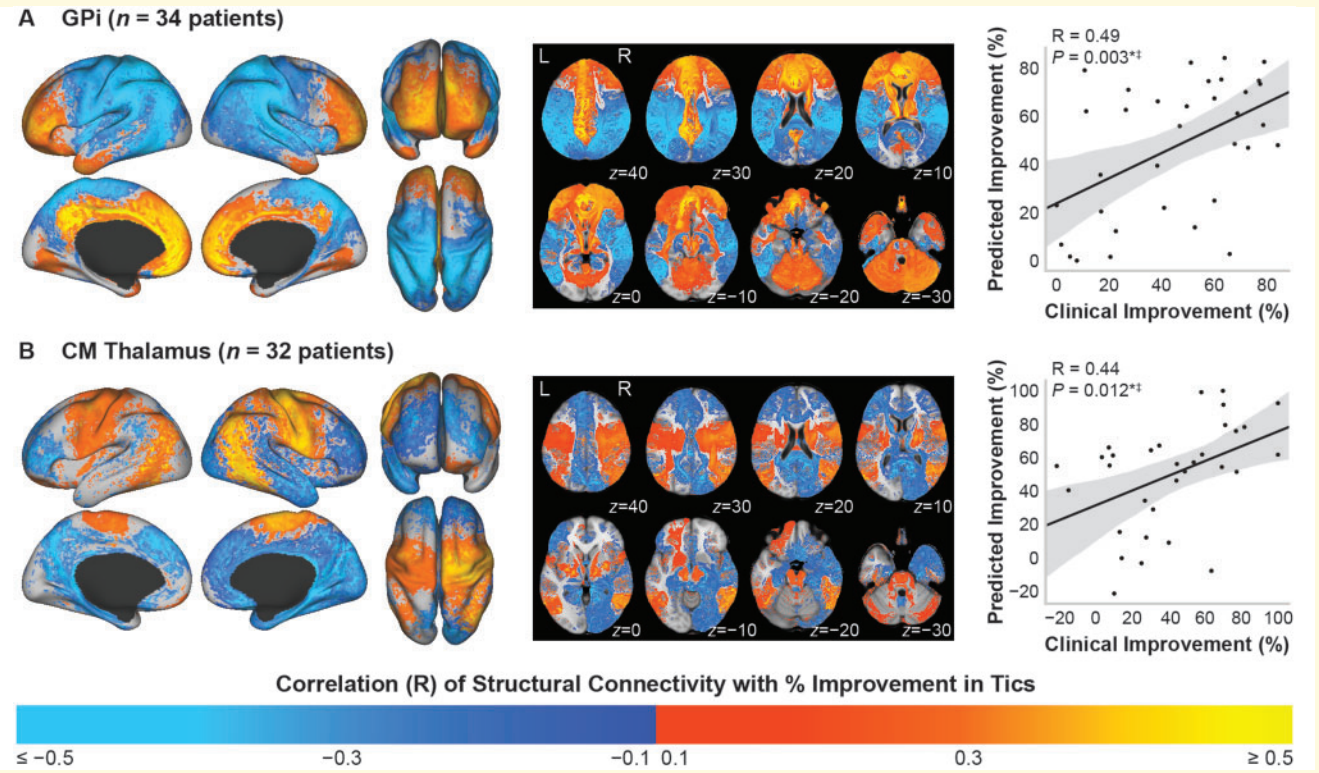

Figure 2 Stimulation-dependent connectivity to structural networks correlated with improvement in tics. Structural connectivity of the VTA correlated with per cent improvement in YGTSS total score. Colour map refers to the correlation coefficient from the voxelwise regression across all patients. (**A**) Across patients implanted in the GPi, connectivity to limbic networks, associative networks, caudate, and cerebellum was positively correlated with tic improvement. Connectivity to sensorimotor networks and parietal-temporal-occipital networks was negatively correlated with improvement. (**B**) Across patients implanted in the centromedial (CM) thalamus, connectivity to sensorimotor networks, parietal-temporal-occipital networks, putamen, and cerebellum was positively correlated with tic improvement. Connectivity to limbic networks and associative networks was negatively correlated with improvement. *Right column:* The predicted improvement scores were significantly correlated with the clinical improvement scores for the GPi and centromedial thalamus, and the models for both targets were robust to leave-one-out cross-validation. *$P < 0.05$; ‡$P < 0.05$ leave-one-out cross-validation.

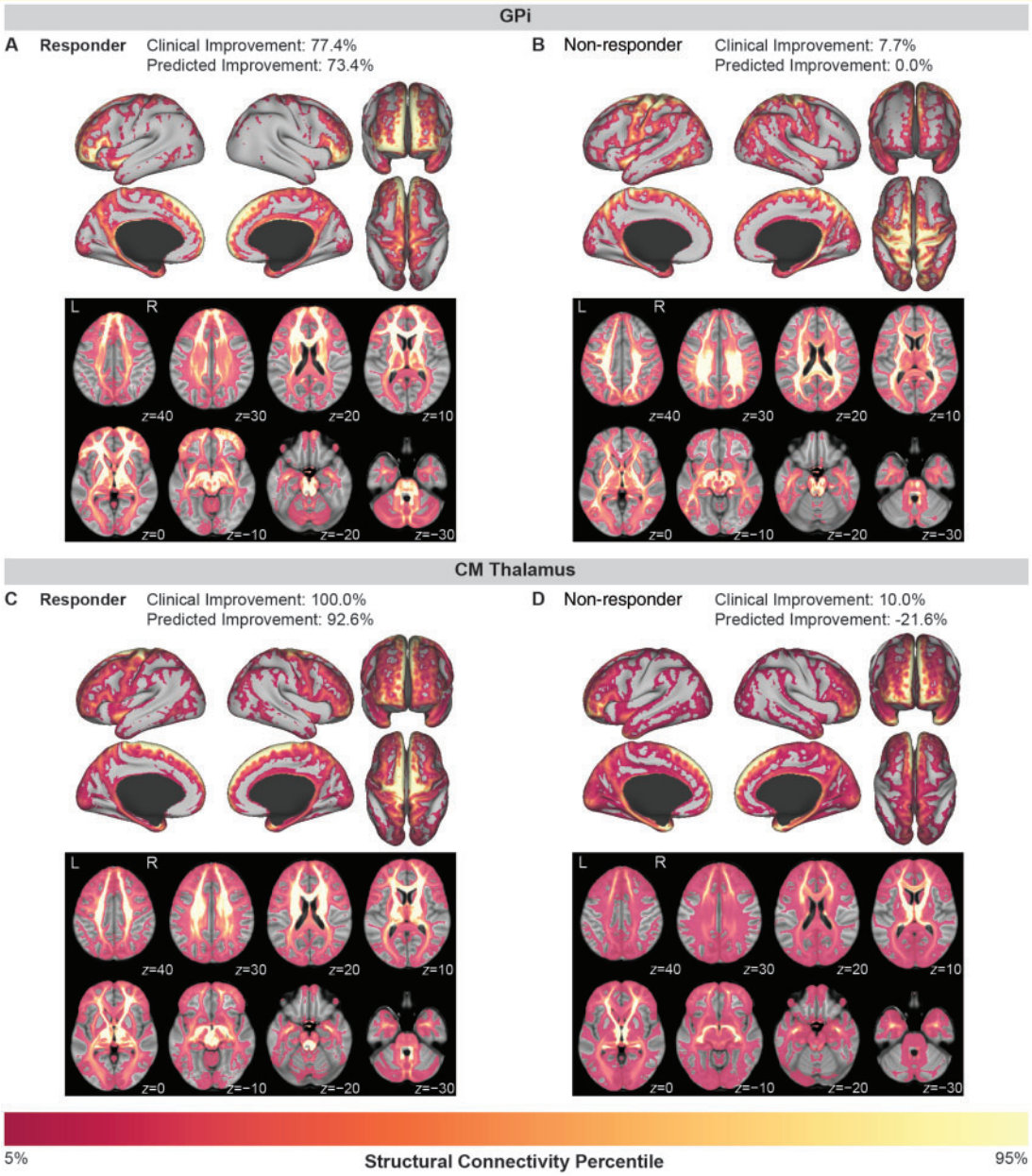

Figure 3 Examples of tic improvement prediction for individual patients implanted in the GPi (*top row*) or the centromedial thalamus (*bottom row*). (**A**) A responder to GPi DBS with 77.4% improvement in tics showed high connectivity to limbic networks (anterior cingulate cortex, orbitofrontal cortex) and associative networks (medial and lateral prefrontal cortex) and low connectivity to sensorimotor networks (primary motor cortex, primary sensory cortex, and premotor areas). (**B**) In contrast, a non-responder to GPi DBS with only 7.7% improvement in tics showed high connectivity to sensorimotor networks and low connectivity to limbic and associative networks. (**C**) A responder to centromedial (CM) thalamus DBS with 100% improvement in tics showed high connectivity to sensorimotor networks (supplementary motor area, motor cortex, and sensory cortex) and lower connectivity to prefrontal and orbitofrontal areas. (**D**) In contrast, a non-responder to centromedial thalamus DBS with only 10.0% improvement in tics showed low connectivity to sensory and motor cortices and higher connectivity to prefrontal and orbitofrontal areas.

temporal-occipital networks. However, for GPi, the model did not significantly predict improvement in OCB [R = 0.39 (95% CI: –0.02 to 0.68), $P = 0.062$]. Additionally, removing the outlier patient implanted in GPi who experienced a 200% worsening of their OCB symptoms resulted in a similar connectivity map to Fig. 4A, and the model still did not significantly predict improvement in OCB [R = 0.34 (95% CI: –0.07 to 0.65), $P = 0.101$]. Although the model across patients implanted in the centromedial thalamus significantly predicted improvement scores [R = 0.53 (95% CI: 0.05 to 0.81), $P = 0.034$], the predicted scores from leave-one-out cross-validation were not significantly correlated with the

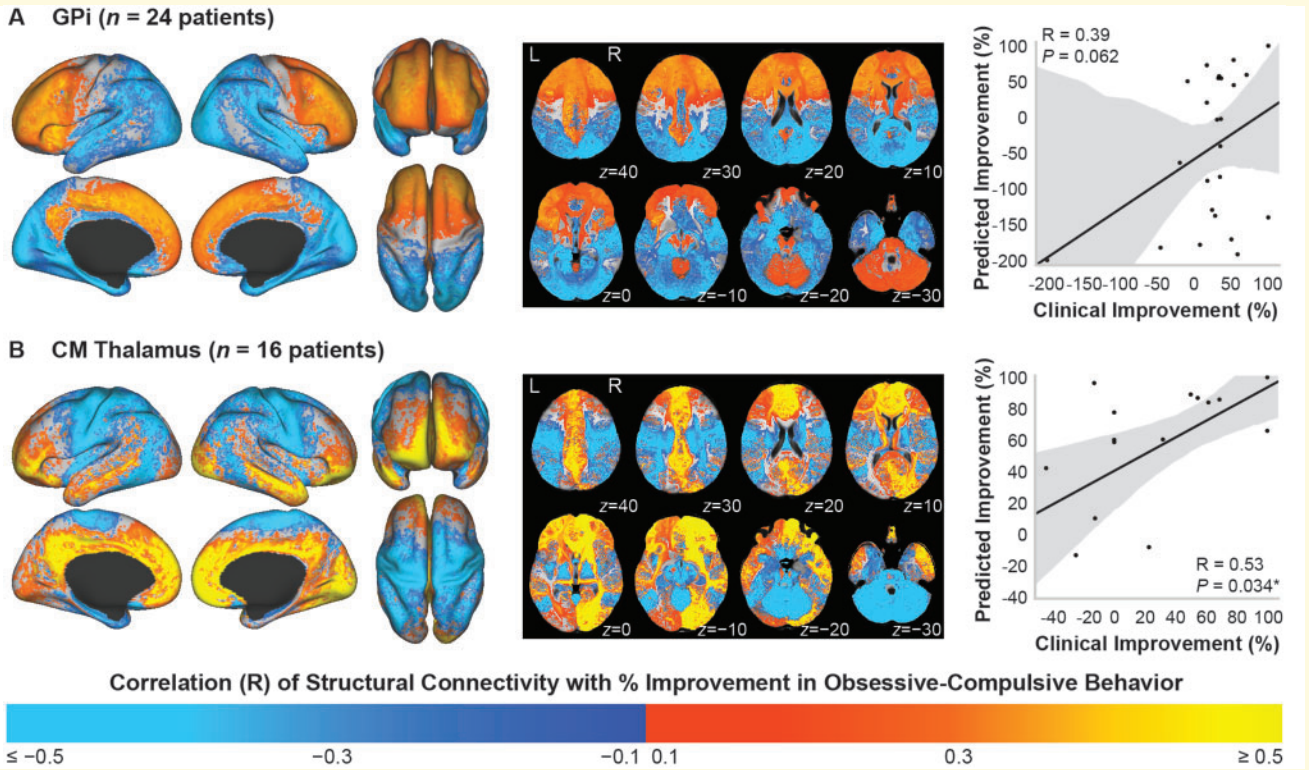

Figure 4 Stimulation-dependent connectivity to structural networks correlated with improvement in OCB. Structural connectivity of the VTA correlated with per cent improvement in Y-BOCS total score in patients implanted in the (**A**) GPi or (**B**) centromedial (CM) thalamus. Colour map refers to the correlation coefficient from the voxelwise regression across patients. Across both targets, connectivity to limbic and associative networks was positively correlated, while connectivity to sensorimotor networks and parietal-temporal-occipital networks was negatively correlated. *Right column:* (**A**) Structural connectivity did not significantly predict clinical improvement across patients implanted in the GPi. (**B**) Structural connectivity significantly predicted improvement across patients implanted in the centromedial thalamus, but the model was not robust to leave-one-out cross-validation. *$P < 0.05$.

clinical improvement scores (R = 0.27, $P = 0.31$). The top correlated regions are visualized in Supplementary Fig. 1C (GPi) and Supplementary Fig. 1D (centromedial thalamus), and regression statistics are summarized in Supplementary Tables 3 and 4. However, because these models did not result in statistically significant predictions for out-of-sample data, the 'reverse' connectivity-based parcellation analyses were not performed for improvement in OCB.

Connectivity-based parcellation of the total stimulation volume

Parcellations based on networks correlated with improvement in tics

Within the total stimulation volume of patients implanted in the GPi, maps of the ratio of the average connectivity to the networks that were positively correlated versus negatively correlated with improvement in YGTSS total scores are shown in Fig. 5. Regions with higher connectivity to positively correlated networks were located in the anterior pallidum and anterior limb of internal capsule (Fig. 5A). Regions with higher connectivity to negatively correlated networks were located in the posterior and ventral pallidum, posterior limb of internal capsule, and ventral to pallidum. The mean ratio value of all voxels within each patient's VTA was significantly correlated with per cent improvement in YGTSS total score in both the left hemisphere [R = 0.41 (95% CI: 0.09 to 0.66), $P = 0.016$] and the right hemisphere [R = 0.41 (95% CI: 0.08 to 0.65), $P = 0.017$] (Fig. 5C).

Among patients implanted in the centromedial thalamus, the parcellation of the total stimulation volume showed that regions with higher connectivity to positively correlated networks were located in lateral regions of the centromedian nucleus (CMn) and regions lateral and ventral to the CMn, parafascicular (pf) nucleus, and ventro-oralis internus (Fig. 5B). A region with particularly high connectivity to negatively correlated networks was located in the right anterior thalamus superior to the ventro-oralis internus (shown in slices $z = 12$ to $z = 8$). However, the mean ratio values for each VTA intersecting with the maps in either the left hemisphere [R = 0.17 (95% CI: −0.19 to 0.49), $P = 0.36$] or right hemisphere [R = 0.22 (95% CI: −0.14 to 0.53), $P = 0.23$] were not significantly correlated with per cent improvement in YGTSS total score (Fig. 5D).

Discussion

The results demonstrate that improvement in tics was correlated with stimulation-dependent connectivity to specific structural networks, and connectivity to the networks predicted the degree of tic improvement and was validated using leave-one-out cross-validation. Different therapeutic networks were correlated with tic improvement across the two DBS targets: the GPi mainly involved limbic and associative networks, while the centromedial thalamus mainly involved sensorimotor and parietal-temporal-occipital networks. A second objective of this study was to utilize these networks to identify local stimulation regions to target or avoid in order to improve tics, and these maps revealed specific regions surrounding the anterior GPi and the lateral/anterior centromedial thalamus that exhibited high connectivity to positively correlated networks. The results also showed trends that OCB improvement may be correlated with structural connectivity to specific prefrontal, orbitofrontal, and cingulate networks. Overall, the results suggest that symptom improvement likely depends on modulation of target-specific therapeutic networks that have been previously implicated in Tourette syndrome and comorbid OCB. Connectivity to these networks could be used to guide DBS targeting and stimulation parameter selection in future Tourette syndrome patients.

Networks correlated with improvement in tics

Modulation of pathophysiological networks

Our results demonstrate that DBS likely improves tics by modulating distributed networks that span multiple functional domains; tic improvement following DBS of the GPi may be caused by modulation of limbic and associative networks, while modulation of sensorimotor networks and parietal-temporal-occipital networks may mediate tic improvement following DBS of the centromedial thalamus (Fig. 2). The networks correlated with tic improvement identified in this study are in agreement with previous studies of the physiological effects of DBS for Tourette syndrome in small cohorts of patients, which reported that DBS modulates activity in specific regions involved in limbic, associative, and sensorimotor networks (such as primary motor and sensory cortices, cingulate cortex, and striatum), as well as parietal-temporal-occipital networks (Haense *et al.*, 2016; Jo *et al.*, 2018).

This is the first study of the networks correlated with tic improvement in a large Tourette syndrome DBS cohort, but the results are in agreement with previous studies of small cohorts showing that several regions involved in limbic, associative, sensorimotor, and parietal-temporal-occipital networks may be correlated with tic improvement (Jo *et al.*, 2018; Brito *et al.*, 2019). Additionally, many regions within the identified networks have been implicated in various aspects of Tourette syndrome pathophysiology, including structural and functional changes, tic expression, premonitory urges, and tic suppression. Structural and functional changes in patients with Tourette syndrome compared to healthy control subjects have been reported in limbic networks (cingulate cortex and orbitofrontal cortex), associative networks (prefrontal cortex), sensorimotor networks (primary motor and sensory cortices, supplementary motor area), and parietal-temporal-occipital regions (Müller-Vahl *et al.*, 2009; Thomalla *et al.*, 2009; Draganski *et al.*, 2010; Worbe *et al.*, 2010, 2015). Other studies of the neural correlates of tic expression have shown that regions in mainly sensorimotor networks (primary motor and sensory cortices), parietal-temporal-occipital networks, and the thalamus are activated upon tic execution (Bohlhalter *et al.*, 2006; Neuner *et al.*, 2014). Premonitory urges, which precede tic expression, have been associated with activity in the cerebellum and putamen, as well as regions in limbic networks (cingulate cortex and anterior insula) and sensorimotor networks (somatosensory cortex, supplementary motor area, premotor cortex) (Bohlhalter *et al.*, 2006; Neuner *et al.*, 2014; Tinaz *et al.*, 2015). Additionally, tic suppression has been linked to basal ganglia structures, regions in associative networks (inferior frontal gyrus and other prefrontal regions), and regions in limbic networks (anterior cingulate cortex) (Peterson *et al.*, 1998; Kawohl *et al.*, 2009; Hong *et al.*, 2013; Ganos *et al.*, 2014). The networks identified in our results are similar to the networks reported to be involved in different phenomena of Tourette syndrome, which suggests that improvement in tics following DBS of GPi or centromedial thalamus is likely mediated through modulating different combinations of these pathophysiological networks. However, it remains unclear whether modulating pathological activity within these networks using DBS improves tics by preventing tic expression, decreasing premonitory urges, or enhancing the ability to suppress tics.

The results of the present study also indicate that different networks are involved in tic improvement following GPi DBS versus centromedial thalamus DBS (Fig. 2), which is especially of interest since the present cohort and other studies have reported similar levels of tic improvement across the two targets (Baldermann *et al.*, 2016; Martinez-Ramirez *et al.*, 2018; Johnson *et al.*, 2019). The inverted networks of GPi versus centromedial thalamus suggest that the mechanisms of tic improvement by DBS may differ across the targets. One potential explanation is that stimulation of GPi may improve tics by decreasing activity in downstream limbic and associative tic-related networks, while stimulation of centromedial thalamus may improve tics by directly disrupting local tic-related pathological activity. Previous studies have shown that GPi stimulation causes temporal locking of neuronal activity with the stimulation pulse, which overrides tic-related activity and increases inhibition of the thalamus and downstream cortical regions (McCairn *et al.*, 2012, 2013; Israelashvili *et al.*, 2015). In contrast, stimulation of centromedial thalamus may reduce tics by directly disrupting pathological activity in the thalamus and downstream sensorimotor networks. This would support the findings of

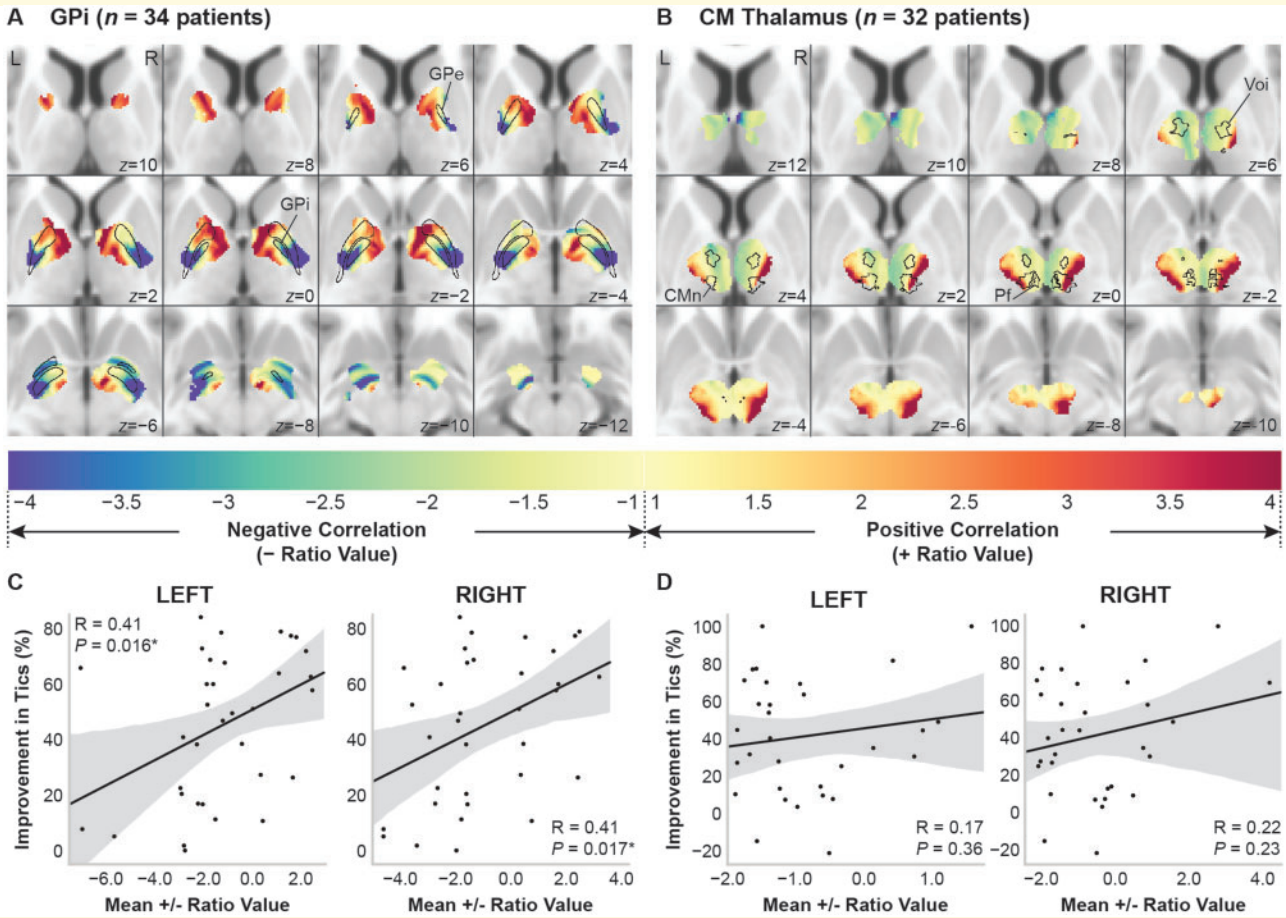

Figure 5 Parcellation of the total stimulation volume across patients into regions based on connectivity to networks correlated with improvement in tics. Maps of the ratio of the average connectivity of positively correlated networks versus the average connectivity of negatively correlated networks for (**A**) patients implanted in the GPi ($n = 34$) and (**B**) patients implanted in the centromedial (CM) thalamus ($n = 32$). Cold colours denote higher connectivity to negatively correlated networks, and warm colours denote higher connectivity to positively correlated networks. (**C** and **D**) The mean ratio value for each patient VTA significantly predicted improvement in YGTSS total score in the GPi (**C**), but not in the centromedial thalamus (**D**). *$P < 0.05$.

neuroimaging and electrophysiological studies reporting that both the thalamus and sensorimotor networks are activated upon tic execution (Bohlhalter *et al.*, 2006; Neuner *et al.*, 2014; Shute *et al.*, 2016; Cagle *et al.*, 2020). Additional studies are needed to uncover these mechanisms and compare the network-level physiological effects of DBS across surgical targets.

Mapping connectivity profiles to stimulated regions

Connectivity-based parcellation for improvement in tics in GPi

The 'reverse' connectivity-based parcellation of the local stimulated regions was particularly of interest as our previous study revealed that VTA location alone was not predictive of clinical outcomes (Johnson *et al.*, 2019). For GPi DBS, the results indicate that stimulation in the anterior pallidum and the anterior limb of the internal capsule likely improves tics by modulating the networks that were positively correlated with improvements in tics, including prefrontal areas and cingulate cortex (Fig. 5). Conversely, stimulation in the posteroventral pallidum and ventral to the pallidum may be less effective at reducing tics due to modulation of negatively correlated networks, including sensorimotor and parietal-temporal-occipital regions. The results also show that overlap of the VTA with the parcellated total stimulation volume map significantly predicted per cent improvement in tics across the cohort. Therefore, these maps could be used to propose stimulation parameters in future patients or potentially revise stimulation parameters for non-responders in order to yield better tic improvement.

Within the present cohort, the posteroventral GPi was the intended target in five patients; however, the spatial distribution of VTAs across patients in our previous study indicated that several of the patients implanted in the anteromedial GPi received stimulation that extended into posteroventral GPi. Our results do not necessarily suggest that all patients

implanted in posteroventral regions of the GPi did not respond to DBS; instead, we hypothesize that the patients who were implanted in the posteroventral GPi and responded to DBS received stimulation that extended into regions that enabled modulation of therapeutic networks. Some studies have reported tic improvement following posteroventral GPi DBS (Martínez-Fernández *et al.*, 2011; Dehning *et al.*, 2014; Zhang *et al.*, 2014), but there has not been an RCT directly comparing the efficacy of anteromedial GPi and posteroventral GPi. However, one case series of six patients suggested that stimulation in the anteromedial GPi may be more effective at reducing tics (Martínez-Fernández *et al.*, 2011). Other studies have suggested that posteroventral GPi DBS may be more suited for patients with specific symptom profiles, including complex motor tics, vocal tics, and self-injurious behaviour (Dehning *et al.*, 2014) or dystonic tics (Kefalopoulou *et al.*, 2015). It remains unclear how to select targets for individual patients, and prospective studies of larger cohorts are needed. However, based on the analysis of the present cohort, stimulation in anteromedial regions of the GPi may yield greater improvement in tics compared to posteroventral regions.

Connectivity-based parcellation for improvement in tics in centromedial thalamus

The map showing the spatial distribution of connectivity to the networks correlated with improvement in tics following centromedial thalamus DBS indicate that some combination of stimulation of lateral CMn and ventral and lateral regions relative to the CMn might yield better improvement in tics by modulating sensorimotor networks and parietal-temporal-occipital networks (Fig. 5). Since VTA overlap did not significantly predict tic improvement in the present study, we cannot conclude that these thalamic subregions are the most effective. However, the trends support the results of studies reporting improvement in tics following DBS of ventral anterior/ventrolateral (VA/VL) motor regions in the thalamus (Huys *et al.*, 2016). Yet, several other studies have reported significant tic improvement following DBS of the CMn-pf complex and the intersection of the CMn-pf and ventro-oralis internus nucleus, including two RCTs (Maciunas *et al.*, 2007; Ackermans *et al.*, 2011).

Specific electrophysiological signatures within the CMn-pf complex and primary motor cortex have also been associated with tics and enable differentiation of tics and voluntary movements (Shute *et al.*, 2016; Cagle *et al.*, 2020). The coupling of CMn-pf complex activity and primary motor cortex activity during tics potentially supports our finding that DBS of the centromedial thalamus likely improves tics through modulation of sensorimotor networks, and these effects are likely not limited to VA/VL motor regions. However, future studies should compare the network-level effects and clinical efficacy of different subregions in the thalamus, perhaps using directional DBS leads (Schüpbach *et al.*, 2017).

Networks correlated with improvement in obsessive-compulsive behaviour

Previous studies of the present cohort and others indicate that DBS can significantly improve psychiatric comorbidities, including OCB (Servello *et al.*, 2016; Johnson *et al.*, 2019). Our results showed that similar connectivity patterns across the two targets were correlated with improvement in OCB (Fig. 4), including positive correlations with connectivity to limbic networks (anterior cingulate cortex, orbitofrontal cortex) and regions across the prefrontal cortex. However, these results should be interpreted with caution because the overall model was not significantly predictive across GPi patients, and the model did not hold up to leave-one-out cross-validation across centromedial thalamus patients. Nonetheless, the reported trends could be used to guide future studies of the effects of DBS on comorbid OCB.

Although this was the first study to investigate the role of stimulation-dependent structural connectivity in mediating improvement in OCB in Tourette syndrome DBS patients, previous studies have reported similar tract activation patterns associated with responders to DBS for obsessive-compulsive disorder (OCD). Studies have found that modulation of specific pathways to the right anterior middle frontal gyrus (Hartmann *et al.*, 2016) and the medial prefrontal cortex (Baldermann *et al.*, 2019) may be crucial for achieving therapeutic responses. Our results indicate that regions in the cingulate cortex were positively correlated with improvement, which is in line with hypothesized mechanisms of DBS for OCD (Bourne *et al.*, 2012; Figee *et al.*, 2013) and agrees with the connectivity pattern found to be predictive of clinical response after anterior limb of internal capsule DBS for OCD (Baldermann *et al.*, 2019). Our findings suggest that DBS may improve OCB in patients with Tourette syndrome by modulating networks that are similar to those targeted with DBS for OCD.

Potential for network-guided neuromodulation

The present study reports novel connectivity-based predictors of clinical outcomes following DBS for Tourette syndrome, which could provide exciting opportunities to guide future studies. Importantly, the leave-one-out cross-validation and example responder and non-responder connectivity maps (Fig. 3) imply that future patients' stimulation-dependent structural connectivity maps could be inputted into the model to give an estimate of their improvement in tics based on lead locations and associated VTAs. Alternatively, the network maps and 'reverse' connectivity-based parcellation maps could be used to test different stimulation parameters for an individual patient based on the overlap of their VTAs. These connectivity maps and 'reverse' connectivity-based parcellation maps could both be combined with recent optimization algorithms (Peña *et al.*,

2017; Anderson *et al.*, 2018) as a means to prospectively select stimulation parameters that optimize the stimulation-dependent connectivity. Stimulation parameter optimization could especially benefit patients whose symptoms are currently not responding to DBS because new stimulation parameters or lead locations could be proposed in order to modulate the therapeutic networks more effectively.

The results of this study may also be important for further developing cortical stimulation or non-invasive stimulation therapies for Tourette syndrome, which have shown variable outcomes across patients, and no RCTs have reported significant reductions in tics compared to sham. However, previous studies have reported trends of improvement following stimulation of the supplementary motor area (Landeros-Weisenberger *et al.*, 2015) and dorsolateral prefrontal cortex (Perani *et al.*, 2018) for Tourette syndrome. Both of these regions were positively correlated with tic improvement in our results, and the reported maps could be used to refine these targets based on connectivity. Further, our results demonstrate that other prefrontal regions may be promising candidate targets for non-invasive stimulation (e.g. deep transcranial magnetic stimulation). The orbitofrontal cortex and cingulate cortex have shown promising results as transcranial magnetic stimulation targets for treating OCD (Berlim *et al.*, 2013; Carmi *et al.*, 2018), and thus these regions may be particularly effective for patients with Tourette syndrome and comorbid OCB.

Limitations

The data from the International Tourette Syndrome DBS Registry and Database were drawn mostly from open-label studies, and therefore the results of this study should be interpreted with caution. Some RCTs have shown that DBS of the anteromedial GPi (Kefalopoulou *et al.*, 2015) and DBS of the centromedial thalamus (Ackermans *et al.*, 2011) significantly reduced tics, while others did not report significant improvement (Welter *et al.*, 2017). RCTs of larger cohorts are needed in order to confirm the efficacy of DBS for Tourette syndrome. However, in this study, we show that utilizing the registry data enabled investigations to study a population that otherwise would be grossly underpowered due to small cohort sizes. Additionally, we opted to analyse data obtained at the latest follow-up time point for each patient instead of a specified time point (e.g. 6 months) in order to maximize the number of patients included in the analysis. This is potentially a limitation because our recent analysis highlighted the importance of time in the response to DBS for Tourette syndrome (Johnson *et al.*, 2019); however, by drawing data from the latest follow-up time point, we are assessing these networks based on the stimulation settings and outcome scores after patients have been stimulated for the longest period of time as available in this retrospective dataset.

Similar to previous studies (Horn *et al.*, 2017; Al-Fatly *et al.*, 2019; Baldermann *et al.*, 2019), the normative connectome approach was used to circumvent using patient-specific DWI, which was not acquired in the vast majority of our patients. As a first step toward understanding which networks were correlated with symptom improvement, we used this approach because it allowed us to pool data from several international centres by using publicly available high-quality imaging. The normative connectome does not account for differences in connectivity due to Tourette syndrome, its comorbidities, or variability between patients. However, previous studies have shown that the predictive models were similar when comparing normative connectomes versus disease-specific or patient-specific connectomes (Horn *et al.*, 2017; Baldermann *et al.*, 2019). This suggests that defining connectivity based on normative data is a reasonable alternative when patient-specific or disease-specific connectomes are not available, which is currently the case for Tourette syndrome. We opted to start with structural connectivity in the present study, and we plan to apply similar methods to functional connectivity in the future to compare against the present results. Additionally, slight spatial errors may be present in the lead location in MNI atlas space; however, we performed careful comparisons of lead locations in patient space versus atlas space, and we specifically excluded any patients whose lead locations were not accurately represented.

Our model was able to account for only some of the variance in clinical outcomes, and therefore other unknown confounding factors that are not network-related are likely important for differentiating responders from non-responders. Furthermore, Tourette syndrome is a highly complex and heterogeneous disorder that is challenging to evaluate, and the YGTSS may be an imperfect proxy for accurately measuring changes in tic severity. In this study, we used the YGTSS total score as an assessment of overall disease severity, which includes an impairment score in addition to the motor and phonic tic severity subscores. Future work will include investigating if specific networks are correlated with improvements in motor versus phonic tics by using these subscales of the YGTSS.

Our methodological approach does not offer any information about whether stimulation causes inhibitory or excitatory effects on distributed networks. Future studies could be designed using simultaneous DBS and functional imaging (Boutet *et al.*, 2019) to investigate whether increased or decreased activity in the networks is associated with symptom improvement. Additionally, the whole-brain tract probability maps do not readily enable the identification of specific white matter tracts. Importantly, it is unclear whether the network-level effects of GPi DBS are mediated through the pallido-thalamic pathways, pallido-subthalamic pathways, or direct cortico-pallidal connections, which are not well understood (Grillner and Robertson, 2016). Future work will be towards identifying specific white matter pathways that may directly connect the target regions to the correlated networks identified in this study. We also note that the VTA is an estimation of the effects of DBS on local tissue, and we used the same medium impedance value for all patients' VTAs, which may over- or under-estimate the VTA

depending on a given patient's actual impedance measurements (Butson *et al.*, 2006). Furthermore, the Hessian VTA method (Anderson *et al.*, 2018) takes all fibre orientations into account and can be used without patient-specific tractography. Future studies could incorporate more complex tract activation models to further test the hypotheses proposed in this study (Lujan *et al.*, 2013).

Conclusions

Stimulation-dependent structural connectivity predicted improvement in tics following DBS targeted to the GPi or centromedial thalamus, and the networks involved across these two targets showed inverted patterns. For GPi DBS, connectivity to limbic and associative networks was positively correlated with tic improvement. Stimulation in the anterior GPi may yield better tic improvement than posterior GPi through modulation of the therapeutic limbic and associative networks, which was in contrast to the posterior GPi that showed higher connectivity to the negatively correlated networks. For centromedial thalamus DBS, connectivity to sensorimotor and parietal-temporal-occipital networks was positively correlated with tic improvement, and regions in the lateral CMn and regions lateral and ventral relative to the CMn-pf complex and ventro-oralis internus showed higher connectivity to these therapeutic networks. For OCB, the connectivity maps were not robust to leave-one-out cross-validation; however, there were similar trends in therapeutic networks across the two targets, which showed that connectivity to the prefrontal, orbitofrontal, and cingulate cortices was positively correlated with OCB improvement. Overall, the structural networks identified in this study could be utilized to refine current neuromodulation targets for Tourette syndrome, or they could be used to propose novel targets that are uniquely positioned to modulate these therapeutic networks in order to improve tics and comorbidities in patients with severe, treatment-refractory symptoms.

Acknowledgements

This study was in collaboration with the Tourette Syndrome Deep Brain Stimulation Working Group; for an updated list of contributing members, please visit the website (https://tourettedeepbrainstimulationregistry.ese.ufhealth.org/). The statistical analyses in this study were supported by the University of Utah Study Design and Biostatistics Center. Data were provided in part by the Human Connectome Project, WU-Minn Consortium (Principal Investigators: David Van Essen and Kamil Ugurbil; 1U54MH091657) funded by the 16 NIH Institutes and Centers that support the NIH Blueprint for Neuroscience Research; and by the McDonnell Center for Systems Neuroscience at Washington University.

Funding

K.A.J. and D.N.A. are supported by the National Science Foundation Graduate Research Fellowship Program (1747505 and 1256065, respectively). K.A.J. and C.R.B. are supported by National Institutes of Health (NIH) P41 Center for Integrative Biomedical Computing (CIBC) (GM103545). G.D., C.R.B., and M.S.O. are supported by NIH NR014852. L.Z. and T.F. are supported by the National Institute for Health Research University College London Hospitals Biomedical Research Centre. The Tourette Association of America provided an International Tourette Syndrome Registry Grant to support this project (PI: M.S.O.). M.S.O. is also supported by NIH R01NS096008. The University of Utah Study Design and Biostatistics Center is funded in part from the National Center for Research Resources and the National Center for Advancing Translational Sciences, National Institutes of Health, through Grant 8UL1TR000105 (formerly UL1RR025764).

Competing interests

J.L.O. has received research grant support from the Michael J. Fox Foundation, Boston Scientific Cala Health, NIH, DARPA, PCORI, and Biogen, and she has also received training grant support from Boston Scientific and Medtronic, and has served as a consultant for Acadia Pharmaceuticals and Medtronic. J.K. has received financial support for Investigator-initiated trials from Medtronic GmbH and grants from the German Research Foundation (KU2665/1-2) and the Marga and Walter Boll Foundation. T.F. has received honoraria for speaking at meetings sponsored by Bill, Profile Pharma and Boston Scientific, and has grant support from National Institute of Health Research, Cure Parkinson's Trust, Michael J Fox Foundation, Innovate UK, John Black Charitable Foundation, Van Andel Research Institute & Defeat MSA. L.Z. acts as a consultant for Medtronic, Boston Scientific & Elekta. A.F.G.L. received a research grant from the Michael J Fox Foundation and royalties from Springer media. A.Y.M. has served as a consultant for Medtronic. L.A. has served as an educational consultant and has participated in advisory board activities for Boston Scientific and Medtronic and has received honoraria for these services. M.S.O. serves as a consultant for the National Parkinson Foundation, and has received research grants from NIH, NPF, the Michael J. Fox Foundation, the Parkinson Alliance, Smallwood Foundation, the Bachmann-Strauss Foundation, the Tourette Syndrome Association, and the UF Foundation. M.S.O. has previously received honoraria, but in the past >60 months has received no support from industry. M.S.O. has received royalties for publications with Demos, Manson, Amazon, Smashwords, Books4Patients, and Cambridge (movement disorders books). M.S. Okun is an associate editor for New England Journal of Medicine Journal Watch Neurology. M.S.O. has participated in CME and educational activities on movement

disorders (in the last 36) months sponsored by PeerView, Prime, QuantiaMD, WebMD, Medicus, MedNet, Henry Stewart, and by Vanderbilt University. The institution and not M.S.O. receives grants from Medtronic, Abbvie, Allergan, and ANS/St. Jude, and the PI has no financial interest in these grants. M.S.O. has participated as a site PI and/or co-I for several NIH, foundation, and industry sponsored trials over the years but has not received honoraria. C.R.B. has served as a consultant for NeuroPace, Advanced Bionics, Boston Scientific, IntelectMedical, St. Jude Medical, Functional Neuromodulation and he holds intellectual property related to DBS.

Supplementary material

Supplementary material is available at *Brain* online.

References

Ackermans L, Duits A, van der Linden C, Tijssen M, Schruers K, Temel Y, et al. Double-blind clinical trial of thalamic stimulation in patients with Tourette syndrome. Brain 2011; 134: 832–44.

Al-Fatly B, Ewert S, Kübler D, Kroneberg D, Horn A, Kühn AA. Connectivity profile of thalamic deep brain stimulation to effectively treat essential tremor. Brain 2019; 142: 3086–98.

Anderson DN, Duffley G, Vorwerk J, Dorval AD, Butson CR. Anodic stimulation misunderstood: preferential activation of fiber orientations with anodic waveforms in deep brain stimulation. J Neural Eng 2019; 16: 016026.

Anderson DN, Osting B, Vorwerk J, Dorval AD, Butson CR. Optimized programming algorithm for cylindrical and directional deep brain stimulation electrodes. J Neural Eng 2018; 15: 026005.

Avants BB, Epstein CL, Grossman M, Gee JC. Symmetric diffeomorphic image registration with cross- correlation: evaluating automated labeling of elderly and neurodegenerative brain. Med Image Anal 2008; 12: 26–41.

Baldermann JC, Melzer C, Zapf A, Kohl S, Timmermann L, Tittgemeyer M, et al. Connectivity profile predictive of effective deep brain stimulation in obsessive-compulsive disorder. Biol Psychiatry 2019; 85: 735–43.

Baldermann JC, Schüller T, Huys D, Becker I, Timmermann L, Jessen F, et al. Deep brain stimulation for Tourette-syndrome: a systematic review and meta-analysis. Brain Stimul 2016; 9: 296–304.

Behrens TEJ, Berg HJ, Jbabdi S, Rushworth MFS, Woolrich MW. Probabilistic diffusion tractography with multiple fibre orientations: what can we gain? Neuroimage 2007; 34: 144–55.

Berlim MT, Neufeld NH, Van den Eynde F. Repetitive transcranial magnetic stimulation (rTMS) for obsessive-compulsive disorder (OCD): an exploratory meta-analysis randomized and sham-controlled trials. Psychiatry 2013; 47: 999–1006.

Bohlhalter S, Goldfine A, Matteson S, Garraux G, Hanakawa T, Kansaku K, et al. Neural correlates of tic generation in Tourette syndrome: an event-related functional MRI study. Brain 2006; 129: 2029–37.

Bourne SK, Eckhardt CA, Sheth SA, Eskandar EN. Mechanisms of deep brain stimulation for obsessive compulsive disorder: effects upon cells and circuits. Front Integr Neurosci 2012; 6: 1–14.

Boutet A, Rashid T, Hancu I, Elias GJB, Gramer RM, Germann J, et al. Functional MRI safety and artifacts during deep brain stimulation: experience in 102 patients. Radiology 2019; 293: 174–83.

Brito M, Teixeira MJ, Mendes MM, França C, Iglesio R, Barbosa ER, et al. Exploring the clinical outcomes after deep brain stimulation in Tourette syndrome. J Neurol Sci 2019; 402: 48–51.

Butson CR, Cooper SE, Henderson JM, McIntyre CC. Patient-specific analysis of the volume of tissue activated during deep brain stimulation. Neuroimage 2007; 34: 661–70.

Butson CR, Cooper SE, Henderson JM, Wolgamuth B, McIntyre CC. Probabilistic analysis of activation volumes generated during deep brain stimulation. Neuroimage 2011; 54: 2096–104.

Butson CR, Maks CB, McIntyre CC. Sources and effects of electrode impedance during deep brain stimulation. Clin Neurophysiol 2006; 117: 447–54.

Cagle JN, Okun MS, Opri E, Cernera S, Molina R, Foote KD, et al. Differentiating tic electrophysiology from voluntary movement in the human thalamocortical circuit. J Neurol Neurosurg Psychiatry 2020; 91: 533–9.

Carmi L, Alyagon U, Barnea-Ygael N, Zohar J, Dar R, Zangen A. Clinical and electrophysiological outcomes of deep TMS over the medial prefrontal and anterior cingulate cortices in OCD patients. Brain Stimul 2018; 11: 158–65.

Dehning S, Leitner B, Schennach R, Ller NMÜ, Tzel K, Obermeier M, et al. Functional outcome and quality of life in Tourette's syndrome after deep brain stimulation of the posteroventrolateral globus pallidus internus: long-term follow-up. World J Biol Psychiatry 2014; 15: 66–75.

Draganski B, Martino D, Cavanna AE, Hutton C, Orth M, Robertson MM, et al. Multispectral brain morphometry in Tourette syndrome persisting into adulthood. Brain 2010; 133: 3661–75.

Duffley G, Anderson DN, Vorwerk J, Dorval AD, Butson CR. Evaluation of methodologies for computing the deep brain stimulation volume of tissue activated. J Neural Eng 2019; 16: 066024.

Van Essen DC, Smith SM, Barch DM, Behrens TEJ, Yacoub E, Ugurbil K. The WU-Minn human connectome project: an overview. Neuroimage 2008; 80: 62–79.

Ewert S, Plettig P, Li N, Chakravarty MM, Collins L, Herrington TM, et al. Toward defining deep brain stimulation targets in MNI space: a subcortical atlas based on multimodal MRI, histology and structural connectivity. Neuroimage 2017; 170: 271–82.

Fan L, Li H, Zhuo J, Zhang Y, Wang J, Chen L, et al. The human brainnetome atlas: a new brain atlas based on connectional architecture. Cereb Cortex 2016; 26: 3508–26.

Fedorov A, Beichel R, Kalphaty-Cramer J, Finet J, Fillion-Robbin J-C, Pujol S, et al. 3D slicer as an image computing platform for the quantitative imaging network. Magn Reson Imaging 2012; 30: 1323–41.

Figee M, Luigjes J, Smolders R, Valencia-Alfonso CE, Van Wingen G, De Kwaasteniet B, et al. Deep brain stimulation restores frontostriatal network activity in obsessive-compulsive disorder. Nat Neurosci 2013; 16: 386–7.

Fischl B. FreeSurfer. Neuroimage 2012; 62: 774–81.

Ganos C, Kahl U, Brandt V, Schunke O, Baumer T, Thomalla G, et al. The neural correlates of tic inhibition in Gilles de la Tourette syndrome. Neuropsychologia 2014; 65: 297–301.

Glasser MF, Stamatios NS, Wilson JA, Coalson TS, Fischl B, Andersson J, et al. The minimal preprocessing pipelines for the human connectome project. Neuroimage 2013; 80: 105–24.

Goodman WK, Price LH, Rasmussen SA, Mazure C, Fleischmann RL, Hill CL, et al. The Yale-Brown obsessive compulsive scale. Arch Gen Psychiatry 1989; 46: 1006–11.

Grillner S, Robertson B. The Basal Ganglia over 500 million years. Curr Biol 2016; 26: R1088–R1100.

Haense C, Müller-Vahl KR, Wilke F, Schrader C, Capelle HH, Geworski L, et al. Effect of deep brain stimulation on regional cerebral blood flow in patients with medically refractory Tourette syndrome. Front Psychiatry 2016; 7: 118.

Hartmann CJ, Lujan JL, Chaturvedi A, Goodman WK, Okun MS, McIntyre CC, et al. Tractography activation patterns in dorsolateral

prefrontal cortex suggest better clinical responses in OCD DBS. Front Neurosci 2016; 9: 519.
Hirschtritt ME, Lee PC, Pauls DL, Dion Y, Grados MA, Illmann C, et al. Lifetime prevalence, age of risk, and genetic relationships of comorbid psychiatric disorders in Tourette syndrome. JAMA Psychiatry 2015; 72: 325–33.
Hong HJ, Sohn H, Cha M, Kim S, Oh J, Chu MK, et al. Increased frontomotor oscillations during tic suppression in children with Tourette syndrome. J Child Neurol 2013; 28: 615–24.
Horn A, Reich M, Vorwerk J, Li N, Wenzel G, Fang Q, et al.. Connectivity Predicts deep brain stimulation outcome in Parkinson disease. Ann Neurol 2017; 82: 67–78.
Horn A, Kühn AA. Lead-DBS: a toolbox for deep brain stimulation electrode localizations and visualizations. Neuroimage 2015; 107: 127–35.
Horn A, Reich M, Vorwerk J, Li N, Wenzel G, Fang Q, et al. Connectivity predicts deep brain stimulation outcome in Parkinson disease. Ann Neurol 2017; 82: 67–78.
Huys D, Bartsch C, Koester P, Lenartz D, Maarouf M, Daumann J, et al. Motor improvement and emotional stabilization in patients with Tourette syndrome after deep brain stimulation of the ventral anterior and ventrolateral motor part of the thalamus. Biol Psychiatry 2016; 79: 392–401.
Israelashvili M, Loewenstern Y, Bar-Gad I. Abnormal neuronal activity in Tourette syndrome and its modulation using deep brain stimulation. J Neurophysiol 2015; 114: 620.
Jo HJ, McCairn KW, Gibson WS, Testini P, Zhao CZ, Gorny KR, et al. Global network modulation during thalamic stimulation for Tourette syndrome. Neuroimage Clin 2018; 18: 502–9.
Johnson KA, Fletcher PT, Servello D, Bona A, Porta M, Ostrem JL, et al. Image-based analysis and long-term clinical outcomes of deep brain stimulation for Tourette syndrome: a multisite study. J Neurol Neurosurg Psychiatry 2019; 90: 1078–90.
Kawohl W, Brühl A, Krowatschek G, Ketteler D, Herwig U. Functional magnetic resonance imaging of tics and tic suppression in Gilles de la Tourette syndrome. World J Biol Psychiatry 2009; 10: 567–70.
Kefalopoulou Z, Zrinzo L, Jahanshahi M, Candelario J, Milabo C, Beigi M, et al. Bilateral globus pallidus stimulation for severe Tourette's syndrome: a double-blind, randomised crossover trial. Lancet Neurol 2015; 14: 595–605.
Klein A, Tourville J. 101 labeled brain images and a consistent human cortical labeling protocol. Front Neurosci 2012; 6: 171.
Landeros-Weisenberger A, Mantovani A, Motlagh MG, De Alvarenga PG, Katsovich L, Leckman JF, et al. Randomized sham controlled double-blind trial of repetitive transcranial magnetic stimulation for adults with severe Tourette syndrome. Brain Stimul 2015; 8: 574–81.
Leckman JF. Tourette's syndrome. Lancet 2002; 360: 1577–86.
Leckman JF, Peterson BS, Anderson GM, Arnsten AFT, Pauls DL, Cohen DJ. Pathogenesis of Tourette's. J Child Psychol Psychiatry 1997; 38: 119–42.
Leckman JF, Riddle MA, Hardin MT, Ort SI, Swartz KL, Stevenson J, et al. The Yale global tic severity scale: initial testing of a clinician-rated scale of tic severity. J Am Acad Child Adolesc Psychiatry 1989; 28: 566–73.
Lujan JL, Chaturvedi A, Choi KS, Holtzheimer PE, Gross RE, Mayberg HS, et al. Tractography-activation models applied to subcallosal cingulate deep brain stimulation. Brain Stimul 2013; 6: 737–9.
Maciunas RJ, Maddux BN, Riley DE, Whitney CM, Schoenberg MR, Ogrocki PJ, et al. Prospective randomized double-blind trial of bilateral thalamic deep brain stimulation in adults with Tourette syndrome. J Neurosurg 2007; 107: 1004–14.
Martínez-Fernández R, Zrinzo L, Aviles-Olmos I, Hariz M, Martinez-Torres I, Joyce E, et al. Deep brain stimulation for Gilles de la Tourette syndrome: a case series targeting subregions of the globus pallidus internus. Mov Disord 2011; 26: 1922–30.
Martinez-Ramirez D, Jiminez-Shahed J, Leckman JF, Porta M, Servello D, Meng F-G, et al. Efficacy and safety of deep brain stimulation in Tourette syndrome The International Tourette Syndrome Deep Brain Stimulation Public Database and Registry. JAMA Neurol 2018; 75: 353–9.
McCairn KW, Iriki A, Isoda M. High-frequency pallidal stimulation eliminates tic-related neuronal activity in a nonhuman primate model of Tourette syndrome. Neuroreport 2012; 23: 206–10.
McCairn KW, Iriki A, Isoda M. Deep brain stimulation reduces tic-related neural activity via temporal locking with stimulus pulses. J Neurosci 2013; 33: 6581–93.
Mink JW. Basal ganglia dysfunction in Tourette's syndrome: a new hypothesis. Pediatr Neurol 2001; 25: 190–8.
Müller-Vahl KR, Grosskreutz J, Prell T, Kaufmann J, Bodammer N, Peschel T. Tics are caused by alterations in prefrontal areas, thalamus and putamen, while changes in the cingulate gyrus reflect secondary compensatory mechanisms. BMC Neurosci 2014; 15: 6.
Müller-Vahl KR, Kaufmann J, Grosskreutz J, Dengler R, Emrich HM, Peschel T. Prefrontal and anterior cingulate cortex abnormalities in Tourette syndrome: evidence from voxel-based morphometry and magnetization transfer imaging. BMC Neurosci 2009; 10: 13.
Neuner I, Werner CJ, Arrubla J, Stocker T, Ehlen C, Wegener HP, et al. Imaging the where and when of tic generation and resting state networks in adult Tourette patients. Front Hum Neurosci 2014; 8: 1–16.
Pedregosa F, Varoquaux G, Gramfort A, Michel V, Thirion B, Grisel O, et al. Scikit-learn: machine learning in Python. J Mach Learn Res 2011; 12: 2825–30.
Peña E, Zhang S, Deyo S, Xiao Y, Johnson MD. Particle swarm optimization for programming deep brain stimulation arrays. J Neural Eng 2017; 14: 016014.
Perani D, Lalli S, Iaccarino L, Alongi P, Gambini O, Franzini A, et al. Prefrontal cortical stimulation in Tourette disorder: proof-of-concept clinical and neuroimaging study. Mov Disord Clin Pract 2018; 5: 499–505.
Peterson BS, Skudlarski P, Anderson AW, Zhang H, Gatenby JC, Lacadie CM, et al. A functional magnetic resonance imaging study of tic suppression in Tourette syndrome. Arch Gen Psychiatry 1998; 55: 326–33.
Rattay F. Analysis of models for external stimulation of axons. IEEE Trans Biomed Eng 1986; BME-33: 974–7.
Rattay F. The basic mechanism for the electrical stimulation of the nervous system. Neuroscience 1999; 89: 335–46.
Schüpbach WMM, Chabardes S, Matthies C, Pollo C, Steigerwald F, Timmermann L, et al. Directional leads for deep brain stimulation: opportunities and challenges. Mov Disord 2017; 32: 1371–5.
Servello D, Zekaj E, Saleh C, Lange N, Porta M. Deep brain stimulation in Gilles de la Tourette syndrome: what does the future hold? A cohort of 48 patients. Neurosurgery 2016; 78: 91–100.
Shute JB, Okun MS, Opri E, Molina R, Rossi PJ, Martinez-Ramirez D, et al. Thalamocortical network activity enables chronic tic detection in humans with Tourette syndrome. Neuroimage Clin 2016; 12: 165–72.
Thomalla G, Siebner HR, Jonas M, Baumer T, Biermann-Ruben K, Hummel F, et al. Structural changes in the somatosensory system correlate with tic severity in Gilles de la Tourette syndrome. Brain 2009; 132: 765–77.
Tinaz S, Malone P, Hallett M, Horovitz SG. Role of the right dorsal anterior insula in the urge to tic in Tourette syndrome. Mov Disord 2015; 30: 1190–7.
Tobe RH, Bansal R, Xu D, Hao X, Liu J, Sanchez J, et al. Cerebellar morphology in Tourette syndrome and obsessive-compulsive disorder. Ann Neurol 2010; 67: 479–87.
Vandewalle V, van der Linden C, Groenewegen HJ, Caemaert J, Linden CVD, Groenewegen HJ, et al. Stereotactic treatment of Gilles de la Tourette syndrome by high frequency stimulation of thalamus. Lancet 1999; 353: 724.

Vorwerk J, Brock AA, Anderson DN, Rolston JD, Butson CR. A retrospective evaluation of automated optimization of deep brain stimulation parameters. J Neural Eng 2019; 16: 064002.

Welter M-L, Houeto J-L, Thobois S, Bataille B, Guenot M, Worbe Y, et al. Anterior pallidal deep brain stimulation for Tourette's syndrome: a randomised, double-blind, controlled trial. Lancet Neurol 2017; 16: 610–9.

Welter ML, Houeto JL, Worbe Y, Diallo MH, Hartmann A, Tezenas Du Montcel S, et al. Long-term effects of anterior pallidal deep brain stimulation for Tourette's syndrome. Mov. Disord 2019; 34: 2018–20.

Worbe Y, Gerardin E, Hartmann A, Valabrégue R, Chupin M, Tremblay L, et al. Distinct structural changes underpin clinical phenotypes in patients with Gilles de la Tourette syndrome. Brain 2010; 133: 3649–60.

Worbe Y, Marrakchi-Kacem L, Lecomte S, Valabregue R, Poupon F, Guevara P, et al. Altered structural connectivity of cortico-striato-pallido-thalamic networks in Gilles de la Tourette syndrome. Brain 2015; 138: 472–82.

Zhang J-G, Ge Y, Stead M, Zhang K, Yan S, Hu W, et al. Long-term outcome of globus pallidus internus deep brain stimulation in patients with Tourette Syndrome. Mayo Clin. Proc 2014; 89: 1506–14.